Bull. Astr. Soc. India (1989) 17, 60-69

Development of a stellar spot model

Praveen Nagar *Department of Astronomy, Osmania University, Hyderabad 500 007*

Received 1989 January 27; accepted 1989 May 1

Abstract. A spectroscopic spot model has been developed incorporating spot magnetic fields. It is shown that the presence of spot magnetic field makes a noticeable effect on the shape of spectral lines.

Key words : stars—starspots—spot modelling

1. Introduction

The present work has mainly been motivated by the spurt of recent research activity in the fields of spotted stars. As far as the late-type stars are concerned the idea of starspot was first given by Kron (1947, 1952) to explain the distortions of the light curves of YY Gem and AR Lac; see Hall (1980) for a review. Vast amount of observational evidence accumulated during this period has turned starspot hypothesis into a well established fact.

Recently a technique called Doppler imaging was introduced by Vogt & Penrod (1983). This technique enables one to get the surface images of spotted stars using high resolution, high signal-to-noise (S/N) spectroscopic data. The basic principle behind the technique is quite simple, i.e., the wavelength positions across the spectral line of a rotating star are directly related to the spatial positions across the projected stellar disc. Any kind of inhomogeneity that occurs on the stellar surface will, therefore, be reflected at the corresponding place in the line profile. As this inhomogeneous region is carried accross the disc due to rotation, the feature related to it in the spectral line will also move accordingly. Such features on late-type spotted stars are now well documented (Fekel 1983, Vogt & Penrod 1983, Gondoin 1986). The Doppler imaging has now become a standard technique in the field of starspot research, though modifications and refinements have been incorporated from time to time in order to make it more reliable.

We have developed a model, similar to the one discussed by Vogt & Penrod (1983) but incorporating the effect of spot magnetic field, with a view to analysing the spectral lines of spotted stars. In the absence of high resolution and high S/N ($\geqslant 400$) data, this paper deals with only the development of the model.

In the following section we describe the method for computing the model atmosphere and intensity line profiles. These profiles are then used by the spot model as described in section 3. The same section deals with a discussion on spot magnetic fields and their effect on the shape of the emergent flux profiles.

2. The model atmospheres and line profiles

The low temperature spots are mainly found in stars of spectral class late F_e to early M. Many of these spotted stars are either on the main sequence or slightly evolved as luminosity class IV. In the RS CVn type systems normally the more evolved component has been found to be the spotted one. We decided to construct the spot model for such luminosity class IV stars. The model, however, can also be applied to other luminosity classes by using the appropriate model atmosphere. The model atmospheres are required for the computations of the line profiles as discussed later. The model atmosphere is constructed with the usual simplifying assumption of a plane parallel geometry, with layers in hydrostatic and radiative equilibrium, i.e., the transport of energy by such hydrodynamical processes as convection is neglected for reasons of tractability. This is perhaps the weakest assumption we have made because we know that in the atmospheres of late-type stars the convection does act as a carrier of energy.

We neglect the fine structure, e.g., granulation, spots etc. The granulation is a manifestation of the turbulence in the atmosphere, and we can introduce the effect of turbulence while computing the line profiles as we do later. Similarly, to introduce the effect of spots on the line we have computed the atmosphere for the spotted region separately.

The magnetic fields are neglected while computing the atmosphere but we included their effect on the lines formed in spots having magnetic fields, through the Zeeman broadening,

Finally we make the assumption of the local thermodynamic equilibrium (LTE), so that excitation, ionization, source function, thermal velocity distribution at any point in the atmosphere are all described by the local temperature. The main sources of continuum opacity considered by us for the model atmosphere are listed below :

(i) Neutral hydrogen bound-free $k(H_{bf})$, (ii) neutral hydrogen free-free $k(H_{ff})$, (iii) negative hydrogen bound-free $k(H^-_{bf})$, (iv) negative hydrogen free-free $k(H^-_{ff})$ (v) negative helium free-free $k(He^-_{ff})$, (vi) metals, and (vii) electron scattering. All the equations required to compute the continuous mass absorption coefficient have been taken from Gray (1976). The chemical composition of the atmosphere relative to hydrogen was taken to be H = 1.0, He = 0.1, and metal abundance as given by Gray (1976) for the sun.

We have computed the model atmospheres for the unspotted and spotted regions separately. For the unspotted region effective temperature was taken to be 5500 K and log of surface gravity as 3.8. This approximately corresponds to a star of G2 IV type. In order to have spots at temperatures 1500 K to 1000 K less than the surrounding atmosphere, we scale down the temperature distribution of the unspotted region by 27% and 23% respectively.

Once a model atmosphere is computed, it can be used for computing theoretical spectral line profiles. Our spot model, described in section 3, requires the emergent intensity profiles at various points on the stellar surface. When combined together these intensity profiles provide the flux profile. The line profiles thus computed were used in our spot model as described below. In the next section we will study the effect of putting spots of various temperatures on the star's surface. We will also consider the effect of magnetic fields in the spots on the shapes of lines produced there. It is shown that this effect should be taken into account while constructing steller surface images by the technique of Doppler imaging.

3. The spot model

3.1. The construction of surface grid

In order to compute a spectral line profile of a spotted star, it becomes necessary to divide the whole stellar surface into a fine grid. This enables one to include the effects of inhomogeneous surface temperature distribution, effects of localized magnetic fields, and of other fine structures into the flux profile emanating from such a surface. Formation of surface grid was accomplished by dividing the projected stellar disc into polar coordinates (r, ϕ). Such a scheme of stellar surface division was used by Khokhlova & Rjabchikova (1975) for computing the line profiles of Ap stars that are known to have abundance patches on their surface. The same technique has been described by Gray (1982) while computing the line profiles of late-type stars to derive their rotational and macroturbulence velocities. We have adopted the method described by Gray for the disc division.

Under this scheme we devide the projected disc into 360 sectors of 1 degree each and 57 annuli. This provides us a total of 20520 area elements on the projected surface. This large number of area elements gives us a better area resolution which is required for accurately defining the spot shape, though the initial testing of the program was done by using only 5040 area elements (i.e., 180 sectors of 2 degree each and 28 annuli). Since the computation time is directly proportional to the number of area elements, the program testing could be completed in almost one fourth of time that was required for the final computations.

3.2. The disc-integration

In order to get the flux profile from the projected disc the first step is to compute the intensity profiles to go along with 57 annuli. Two separate data files were created, one for the lines produced in the unspotted region and the other for those produced in the spots. The spot parameters, e.g., its shape and position (longitude and latitude) were stored in a third file. The disc-integration starts from the limb, i.e., from the 1st sector of the 1st annulus. The intensity profile corresponding to that particular area element is first Doppler shifted before being added to the intensity profile of the next area element and so on. This way the disc-integration gradually spirals down to the centre of the disc. During the disc-integration, if a

spot is encountered, the program opens the file containing the intensity profiles produced in spots and picks out the appropriate intensity profile to be used.

If v is the equatorial rotational velocity of the star and i the inclination of its rotational axis to the line of slight, then line of sight velocity of an area element is given by

$$v' = r.v \sin i \cos \phi, \qquad ...(1)$$

where r is fractional radius of the projected disc and ϕ the azimuthal angle. Therefore, the flux profile obtained by the disc-integration can be written as

$$F'_v(0) = \oint I'_v(\theta) \cos \theta \, dw. \qquad ...(2)$$

Here $I'_v(\theta)$ is the Doppler shifted intensity profile; dw the solid angle : $dw = \sin(\theta)\, d\theta d\phi$; and the integration has been carried out over the whole disc. The equation (2) is valid only if the profile is rotationally broadened. If macroturbulence is present then we can convolve the above rotationally broadened profile by a macroturbulence function $\circledR(\Delta\lambda)$. This will give a profile broadened by both rotation as well as macroturbulence. The broadening due to the microturbulence is already included while computing the intensity profile. For the time being we will ignore macroturbulence and take into account only rotation as it is the major source of line broadening.

For simplicity we have considered the spots to be circular in shape. Spots of irregular shape can be accommodated using Strassmeier's (1988) technique which involves digitization of the image.

We now show how a line profile appears for different ΔT values. Here ΔT stands for the difference between the unspotted region and the spotted region temperatures.

3.3. Profile shapes for different ΔT

We have taken a circular, circumpolar spot of radius 20° on a star with its axis of rotation inclined at an angle of 30° to the line of sight. We compute the profiles at four different phases 0, 0.3, 0.5, and 0.8. This is sufficient to show the behaviour of change in projected spot area on the profiles as well. The zero phase corresponds to the situation when the projected spot area is a maximum. The absorption line selected for computation was λ6237.33 due to Si I. In fact we could use almost any neutral absorption line. We have further taken the projected rotation velocity, $v \sin i$, of the star as 30 km s^{-1}. In figure 1 we show the profiles computed for three different values of ΔT : $\Delta T_{max} = 5500$ K, $\Delta T = 1500$ K, and $\Delta T = 1000$ K. ΔT_{max} corresponds to the situation when the spot temperature is zero and therefore, there is absolutely no light coming out of it. Although in reality such a situation does not exist, it tells us about the maximum amount of distortion that can occur in a line profile for a given size of the spot. The other two values of ΔT are within the range found by many authors by mainly photometric modelling of the light curves.

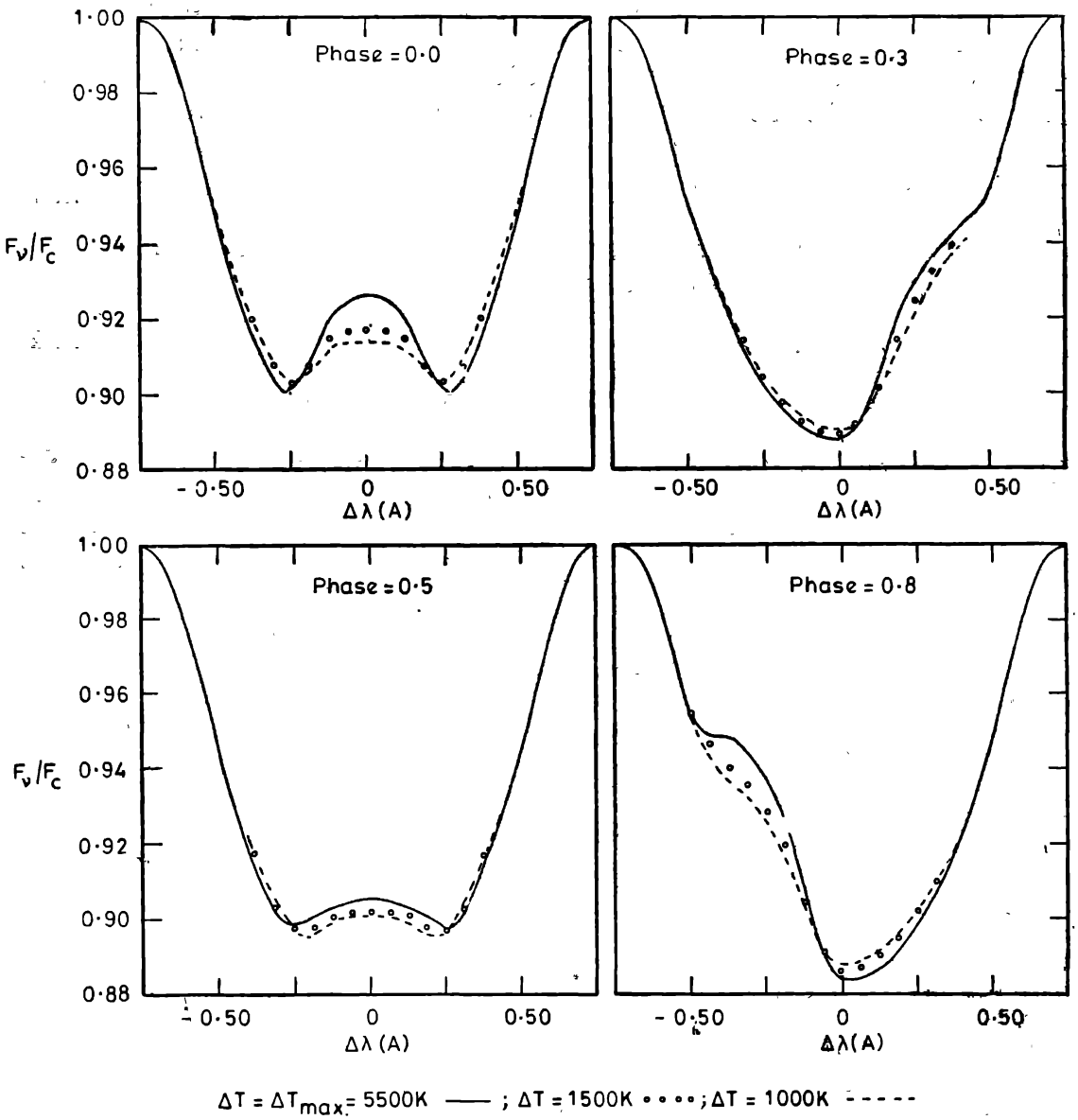

Figure 1. The absorption line profiles corresponding to four phases. The solid line corresponds to $\Delta T = \Delta T_{max}$, the open circles to $\Delta T = 1500\ K$ and dashed line to $\Delta T = 1000$ K. The reduction in the size of the apparent emission bump due to the increase in the spot temperature can be seen at all the phases.

Figure 1 clearly shows that the size of the bump or distortion in the profile is coupled with the temperature difference between the spot and surrounding photosphere as well as the projected area of the spot. As ΔT becomes smaller and smaller, the profile tends to return to its normal shape. Similar behaviour is seen with the variation of projected spot area, i.e., as the area coverage by the spot reduces, the line profile again approaches its normal shape. The spot in our model is of moderate size, only 20° in angular radius covering $\approx 6\%$ of the visible surface. Although spots of angular radius 40° to 70° have been deduced

for some stars, e.g., II Peg and BY Dra (Vogt 1981b), inspite of our choice of a smaller spot we see that the effect of different spot temperature is quite noticeable on the profiles. We found the same thing when we introduced the magnetic field in the spot. The other parameters like star's inclination, the longitude, and latitude of the spot also affect the profile in similar fashion. But, since the variation of any of these parameters changes the projected spot area, we can say that the final shape of the line profile is mainly determined by the ΔT and the area coverage by the spot.

This was perhaps the main reason why all the investigators from 1983 till 1988 ignored the presence of magnetic fields in and around the spotted regions. Despite all the observational evidence (Robinson *et al.* 1980; Marcy 1984; Gray 1984; Vogt 1981a, 1982; Geyer & Metz 1977), no one has earlier tried to incorporate the spot's magnetic fields in the model for Doppler imaging.

3.4. Inclusion of spot magnetic fields in the model

In order to incorporate the magnetic fields, we follow the procedure of Zeeman splitting of spectral lines in the spots. We assume the spot magnetic field lines to be perpendicular to the stellar surface. In the sunspots, field lines are known to be perpendicular to the surface at the centre of the spot but are inclined at an angle of approximately 70° at the edges (Bray & Loughhead 1964). We, however, assume the field lines to be normal all across the spot surface for simplicity.

A Zeeman broadened profile can be approximately represented by the sum of three components, the unshifted component I_π and two shifted components denoted by I_σ. Following Gray (1984) we can write the relative intensities of these components as

$$I_\pi = 0.5 \sin^2 \theta, \qquad \ldots(3)$$

and

$$I_\sigma = 0.25 (1 + \cos^2 \theta), \qquad \ldots(4)$$

where θ is the angle between the magnetic field lines and the line of sight. The shift of the σ components is given by

$$\Delta\lambda = 4.67 \times 10^{-13} \lambda^2 \bar{g} B, \qquad \ldots(5)$$

where λ is the wavelength of the line of interest, $\bar{g}$ is the Lende-g factor, and B is the magnetic field strength in gauss. Therefore, the emergent intensity profile from an atmosphere having a uniform magnetic field is given by (Title & Tarbell 1975; Robinson 1980; Marcy 1982)

$$I(\lambda) = I_\pi \phi(\lambda) + I_\sigma [\phi(\lambda + \Delta\lambda) + \phi(\lambda - \Delta\lambda)], \qquad \ldots(6)$$

where $\phi(\lambda)$ represent the shape of the Zeeman components. For $\phi(\lambda)$ we use the unbroadened intensity profile itself.

The shift $\Delta\lambda$ does not depend only on $\bar{g}$, even though it is an indicator of magnetic sensitivity of the line. $\Delta\lambda$ also depend on λ^2 as well as on B. Longer wavelengths and high magnetic fields can produce large shifts in the lines even though $\bar{g}$ may be small. Fields of the order of 10 to 20 kilogauss in the spots

have been suggested (e.g., Mullan 1974, 1975; Mullan & Bell 1976). This means that even a Zeeman insensitive line, e.g., λ6237.33 ($\bar{g} = 0.75$), will show a broadening of 136 mÅ for a field of 10 kilogauss. Even if we assume that Mullan has overestimated the field strength in the spot, we still get a broadening of more than 65 mÅ for this line with a more realistic value of magnetic field of 5 kilogauss. Broadening of 65 mÅ or more is well within the range of detection with the present-day instruments and techniques. This example strengthens our argument in favour of inclusion of Zeeman splitting while analysing the lines for Doppler imaging irrespective of whether we use Zeeman sensitive lines or not. The final broadening will depend on the combination of magnetic field strength, the wavelength and the Lande-g factor.

3.5. Profile shape for different B

In order to see the effect of different magnetic field strengths in the spot on the line shapes, we repeat the computations done in the section 3.3 for $\Delta T = 1500$ K and 1000 K taking the spot field strength to be 2, 4, and 6 kilogauss. For $\Delta T = \Delta T_{max}$ the computation is meaningless since there would not be line formation in spot, as the spot temperature is zero in this case, so the question of Zeeman splitting does not arise here. But the results for other two values of ΔT are shown in figures 2a and 2b for zero phase, i.e., at the time of maximum area coverage by the spot. For comparison we have also plotted the profile obtained without the spot magnetic field. Figures 2a and 2b clearly show that the presence of magnetic fields in the spots does alter the profile shape. The height of emission bump goes down progressively with the increase in the magnetic field strength.

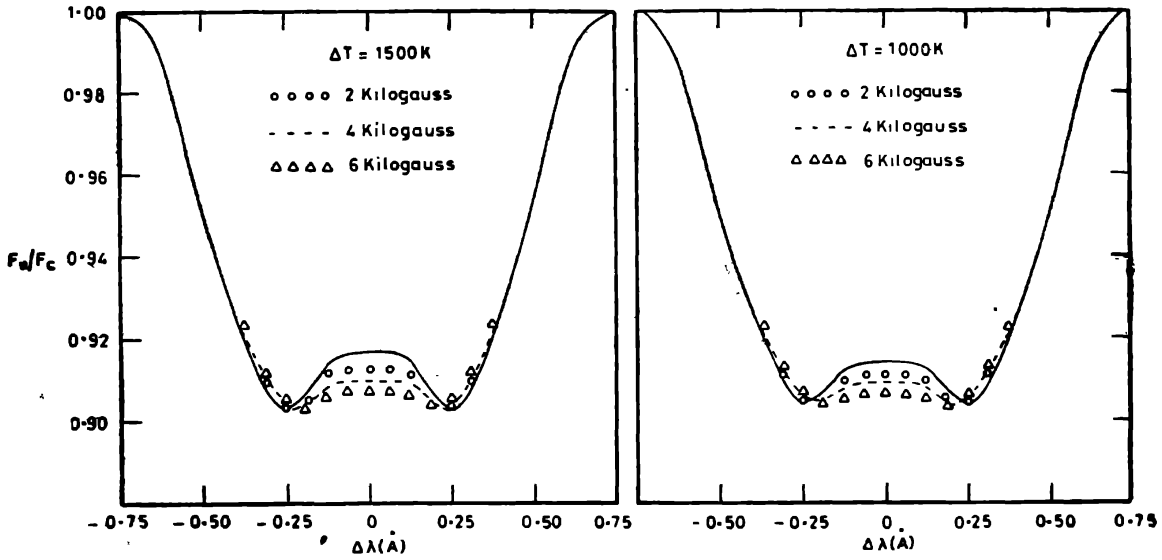

Figure 2. The effect of introducing spot magnetic field is shown here for two ΔT values : (a) for $\Delta T = 1500$ K and (b) for $\Delta T = 1000$ K. In both the cases the effect of spot magnetic field of 2, 4, and 6 kilogauss on the emission bump is noticeable. The open circles are for 2 kilogauss spot field, dashed line is for 4 kilogauss and the triangles are for 6 kilogauss field. For comparison a profile for no spot magnetic field is also shown by a solid line.

This behaviour is similar to the effect of increasing the spot temperature. In the Doppler imaging it is the shape of the profile that is used in deriving stellar surface image. If the distortions caused by spot magnetic field are not taken into account or interpreted as only due to temperature difference between the spot and the surrounding photosphere, then this will results in a wrong determination of various spot parameters. We, therefore, suggest that while modelling the spectral line profiles of spotted stars, one must properly take into account the spot magnetic field, even though an assumption regarding field orientation will be required.

3.6. Inclusion of broadening due to macroturbulence

In section 3.2 we mentioned that the broadening due to macroturbulence can also be included in the profile. One way of doing so is to incorporate it in the intensity profiles used for disc-integration, i.e., all the 57 intensity profiles should be convolved with an appropriate macroturbulence function. We decided not to adopt this procedure as it would have required a total of 57 convolutions. Instead we computed the flux profile (broadened by thermal and rotational broadening) and made a single convolution with an isotropic macroturbulence function. However, nowadays an anisotropic model for the macroturbulence, due to Gray (1976), is more popular. The profiles without macroturbulence and with Gaussian macroturbulence velocity distribution ($G_G = 4$ km s^{-1}) plotted in figure 3 on top of each other. The right-hand side panel of figure 3 also shows the Gaussian macroturbulence profile for $G_G = 4$ km s^{-1} with which the disc-integrated profile was convolved. We clearly see that the rotational broadening dominates the macroturbulence broadening here.

4. Conclusions

In this paper we have reported the progress made towards developing a spot model along the lines of the one described by Vogt & Penrod (1983), by incorporating an additional parameter, i.e., the spot magnetic field. We show that the presence of spot magnetic field does change the shape of the emergent flux profile. This effect is maximum when the spot is crossing the meridian and when the rotational broadening is not too large. We also show that the effect of increasing the spot magnetic field mimics the effect of increasing the spot temperature. We still do not know of a way to decouple the two effects. While introducing the Zeeman broadening due to the magnetic fields we assumed the field lines to be normal to the spot surface. We cannot make any better assumption in the absence of knowledge of field morphology in the starspots, but our assumption seems to be a reasonable one if we take an analogy with the orientation of sunspot field lines that are normal to the spot surface for most part of it.

In future we plan to incorporate more realistic model atmosphere computations with an anisotropic macroturbulence function, e.g., radial-tangential macroturbulence.

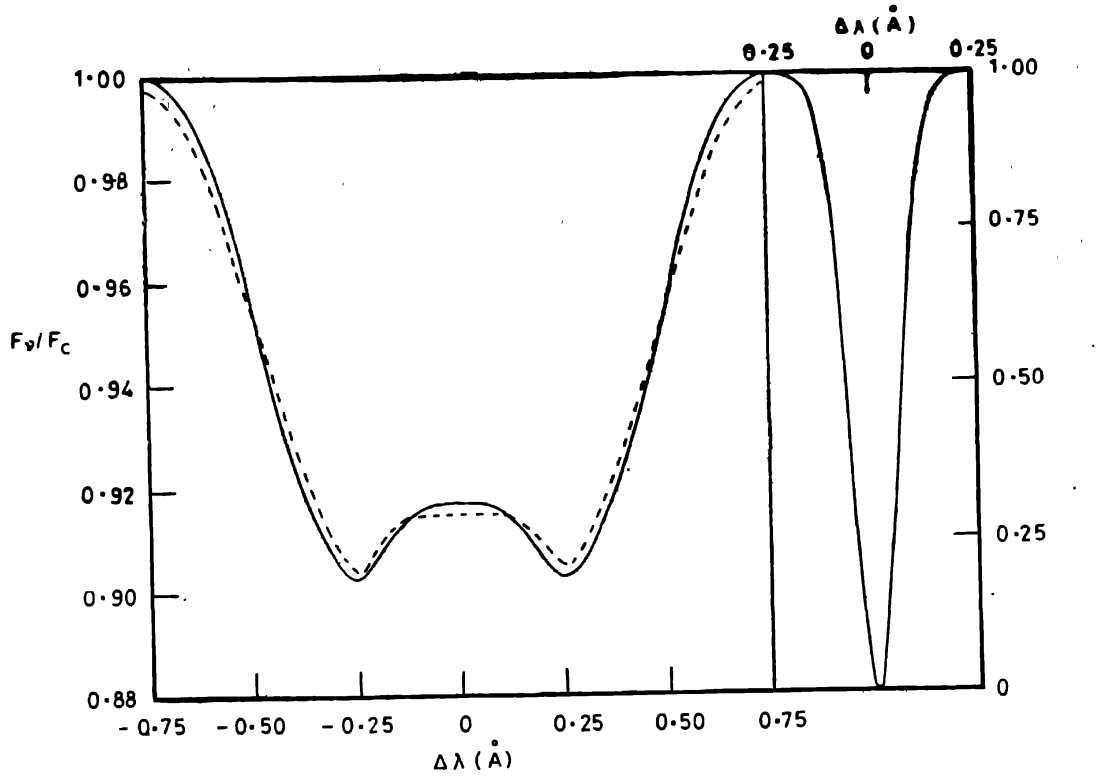

Figure 3. The effect of adding a Gaussian macrotubulence dispersion of 4 km s^{-1} to the purely rotationally broadened profile is shown here. The effect of adding macroturbulence is very small as rotation is the major source of line broadening. Profile with solid line is for pure rotation and the profile shown by dashed line includes rotation and macroturbulence both. The side panel shows the unit height Gaussian macroturbulence profile with which the original flux profile was convolved.

Acknowledgements

I thank Prof. K. D. Abhyankar for many useful comments and suggestions. Thanks are also due to the government of India's department of science and technology, New Delhi, for financial support.

References

Bray, R. J. & Loughhead, R. E. (1964) *Sunspots*, Chapman & Hall, p. 210.
Fekel, F. J. (1983) *Ap. J.* **268**, 274.
Geyer, E. H. & Metz, K. (1977) *Ap. Sp. Sci.* **52**, 351.
Gray, D. F. (1976) *The observation and analysis of stellar photosphere*, Wiley-Interscience.
Gray, D. F. (1982, 1984) *Ap. J.* **258**, 201; **277**, 640.
Gondoin, P. (1986) *Astr. Ap.* **160**, 73.
Hall, D. S. (1980) in *Highlights of Astronomy* **5**, 841.
Khokhlova, V. L. & Rjabchikova, T. A. (1975) *Ap. Sp. Sci.* **34**, 403.
Kron, G. E. (1947, 1952) *Publ. Astr. Soc. Pacific* **59**, 261; *Ap. J.* **115**, 301.
Marcy, G. W. (1982, 1984) *Publ. Astr. Soc. Pacific* **94**, 562; *Ap. J.* **276**, 286.
Mullan, D. J. (1974, 1975) *Ap. J.* **192**, 149; *Astr. Ap.* **40**, 41.
Mullan, D.J. & Bell, R. A. (1976) *Ap. J.* **204**, 818.

Robinson, R. D. (1980) *Ap. J.* **239,** 361.
Robinson, R. D., Worden, S. P. & Harvey, J. W, (1980) *Ap. J.* (*Lett.*) **236,** L155.
Strassmeier, K. G. (1988) *Ap. Sp. Sci.* **140**, 223.
Title, A. M. & Tarbell, T. D. (1975) *Solar Phys.* **41**, 255.
Vogt, S. S. (1981a, b) *Ap. J.* **247**, 975; **250**, 327.
Vogt, S. S. (1982) *IAU Coll. No.* 71, p. 137.
Vogt, S. S. & Penrod, G. D. (1983) *Publ. Astr. Soc. Pacific* **95,** 565.